Available online at www.sciencedirect.com
ScienceDirect
Applied Surface Science 253 (2007) 9248–9253
applied surface science
www.elsevier.com/locate/apsusc

The effects of hydrogen plasma pretreatment on the formation of vertically aligned carbon nanotubes

Wen-Pin Wang [a], Hua-Chiang Wen [a], Sheng-Rui Jian [b,*], Jenh-Yih Juang [b,c], Yi-Shao Lai [d], Chien-Huang Tsai [e], Wen-Fa Wu [f], Kuan-Ting Chen [a], Chang-Pin Chou [a]

[a] *Department of Mechanical Engineering, National Chiao Tung University, Hsinchu 300, Taiwan*
[b] *Department of Electrophysics, National Chiao Tung University, Hsinchu 300, Taiwan*
[c] *Department of Physics, National Taiwan Normal University, Taipei 106, Taiwan*
[d] *Central Labs, Advanced Semiconductor Engineering, Inc. 26 Chin 3rd Rd., Nantze Export Processing Zone, 811 Nantze, Kaohsiung, Taiwan*
[e] *Department of Automation Engineering, Nan Kai Institute of Technology, Nantou 54243, Taiwan*
[f] *National Nano Device Laboratories, Hsinchu 300, Taiwan*

Received 5 March 2007; received in revised form 23 May 2007; accepted 23 May 2007
Available online 2 June 2007

Abstract

The effects of H_2 plasma pretreatment on the growth of vertically aligned carbon nanotubes (CNTs) by varying the flow rate of the precursor gas mixture during microwave plasma chemical vapor deposition (MPCVD) have been investigated in this study. Gas mixture of H_2 and CH_4 with a ratio of 9:1 was used as the precursor for synthesizing CNTs on Ni-coated TiN/Si(1 0 0) substrates. The structure and composition of Ni catalyst nanoparticles were investigated by using scanning electron microscopy (SEM) and cross-sectional transmission electron microscopy (XTEM). Results indicated that, by manipulating the morphology and density of the Ni catalyst nanoparticles via changing the flow rate of the precursor gas mixture, the vertically aligned CNTs could be effectively controlled. The Raman results also indicated that the intensity ratio of the G and D bands (I_D/I_G) is decreased with increasing gas flow rate. TEM results suggest H_2 plasma pretreatment can effectively reduce the amorphous carbon and carbonaceous particles and, thus, is playing a crucial role in modifying the obtained CNTs structures.
© 2007 Elsevier B.V. All rights reserved.

PACS : 61.46.+w; 68.37.Hk; 68.37.Lp; 81.20.−n

Keywords: Carbon nanotubes; H_2 pretreatment; Raman spectroscopy; Scanning electron microscopy; Transmission electron microscopy

1. Introduction

Carbon nanotubes (CNTs) undoubtedly have become one of the most studied advanced materials because of their novel electrical, mechanical and chemical characteristics. Potential applications harvesting the unique properties of CNTs have already been explored in fields such as the field-effect transistor [1], sensor [2,3], field emission display [4,5] and nanoscale interconnects [6].

Many methods have been developed to prepare the catalysts and to grow the CNT, such as high pressure arc [7], laser ablation [8], thermal chemical vapor deposition (CVD) [9] and plasma-enhanced CVD (PECVD) [10], reasonably to control the catalysts; sizes and densities of CNTs are decided by those of the catalysts. Among these, PECVD methods are particularly attracting due to their specificities, for example vertical alignment of CNTs production, low synthesis temperature as compared to arc, laser ablation, CVD, etc., and well-controlled as patterned for nanotubes [11–17]. On the other hand, long and dense arrays of aligned CNTs can readily be obtained by CVD processes [18,19]. Consequently, CVD has become one of the prominent methods to synthesize high purity, high yield CNTs for practical applications.

Nevertheless, depending on the detailed process parameters, the structure of the obtained CNTs and, hence, their associated electronic and mechanical properties are diversified and, sometimes, controversial. There have been several attempts in trying to control the structure of CNTs by methods including

* Corresponding author.
E-mail address: srjian@gmail.com (S.-R. Jian).

0169-4332/$ – see front matter © 2007 Elsevier B.V. All rights reserved.
doi:10.1016/j.apsusc.2007.05.060

the pretreatment of the metal films used for CNTs growth or direct control of structure by varying synthesis parameters [20–28]. For the former, the plasma etching transformed the metallic catalytic layer into catalytic nanoparticles and was applied to control the density of CNTs [29]. However, in order to avoid the formation of metal silicide at high temperatures, buffer layer was adopted in the annealing process [21]. Herein, the effects of H_2 plasma pretreatment on the growth morphology and structure of CNTs synthesized on Ni/TiN/Si substrates by using the microwave plasma chemical vapor deposition (MPCVD) method are systematically investigated in this article.

2. Experimental details

The substrates used in the experiments were 6-in. p-Si(1 0 0) wafers, which were cleaned by using the RCA standard clean procedures to remove chemical impurities and particles. The RCA clean is the industry standard for removing contaminants from wafers. Here, the RCA cleaning procedure has three major steps used sequentially: (I) Organic Clean: removal of insoluble organic contaminants with a 5:1:1 H_2O:H_2O_2:NH_4OH solution; (II) Oxide Strip: removal of a thin silicon dioxide layer where metallic contaminants may accumulate as a result of (I), using a diluted 50:1 H_2O:HF solution; and (III) Ionic Clean: removal of ionic and heavy metal atomic contaminants using a solution of 6:1:1 H_2O:H_2O_2:HCl.

A 20-nm thick layer of TiN followed by a 7-nm thick layer of Ni was deposited on the cleaned substrate with a power of 800 W at a sputtering pressure of 6.4×10^{-3} Torr. A 915 MHz microwave plasma chemical vapor deposition (MPCVD) system was used to grow CNTs. The base pressure of the system was better than 2×10^{-3} Torr. During the growth of CNTs, the substrates were heated using a graphite heater. The experiment details are as follows: first, we obtained the Ni-coated substrates (Ni/TiN/Si) from PVD deposition and second, the Ni-coated substrate processed via H_2 plasma pretreatment at 550 °C for 10 min with various H_2 flow rates, namely 200, 300 and 400 sccm. Herein, the Ni catalyst layer was converted into nanoparticles, which were examined by the scanning electron microscopy (SEM, Hitachi S-4000) and the high-resolution transmission electron microscopy (HRTEM, JEOL, JEM-2100F). Third, as pretreatment finished, then for the synthesis of CNTs a H_2:CH_4 = 9:1 gas mixture was introduced into the chamber at 550 °C for 10 min prior to deposition. In our MPCVD system, the substrate was heated directly by a resistively heated graphite stage and its temperature was measured using a thermocouple attached directly to the upper surface of the stage. The total pressure in the chamber was kept at 20 Torr while the gas flow rates, which were controlled

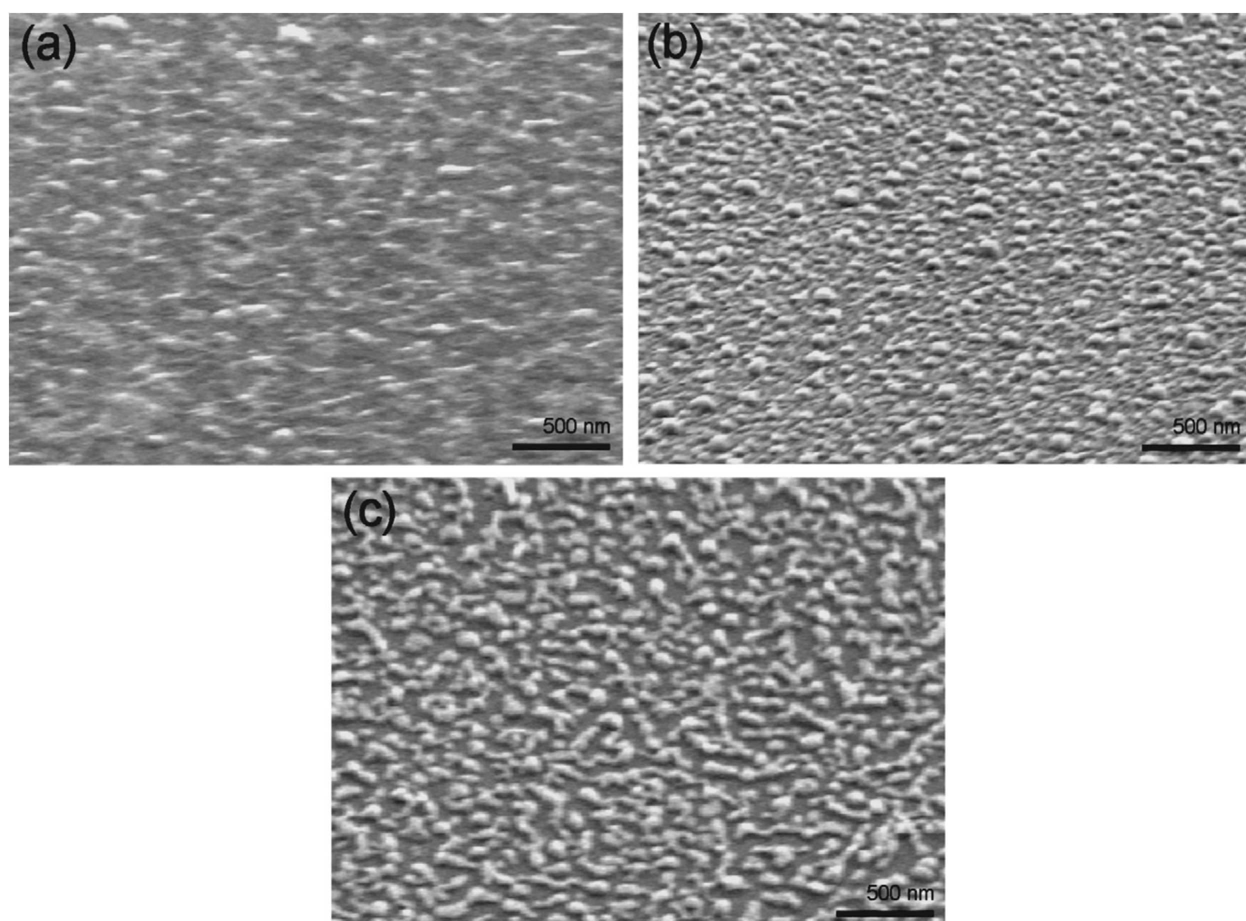

Fig. 1. SEM images of Ni catalyst nanoparticles at the various H_2 plasma pretreatment flow rates of (a) 200, (b) 300 and (c) 400 sccm.

independently using separate mass flow controllers, were increased from 200 to 400 sccm. The obtained aligned CNTs were investigated by means of SEM, TEM techniques. In addition, a Renishaw-1000 Raman spectroscopy equipped with a charge coupled device detector, operating at a wavelength of 514.5 nm and a power of 100 mW, was employed to characterize the crystalline quality of the obtained CNT films.

3. Results and discussion

The synthesis of CNTs by CVD often involves three main steps: (i) decomposition of hydrocarbon gas at the surface of catalyst nanoparticles; (ii) diffusion of resultant carbon atom in the nanoparticles to form the nucleation seed; and (iii) precipitation of carbon atoms at the nanoparticles interface to form CNTs. As a result, the size and chemical composition of metal nanoparticles have been considered as the dominant factors in determining the diameter and structural perfection of CNTs [16]. Thus, as the first step of this investigation, we examined the effect of H_2 plasma pretreatment on the Ni metal catalyst layer sputtered on TiN coated Si substrate. As is illustrated in Fig. 1, the Ni metal catalyst layer was transformed into nanoparticles after the H_2 plasma pre-treatment, and the size and distribution of these nanoparticles are very much dependent on the flow rate of H_2 during plasma pretreatment. In addition, from the SEM observations, it appears that higher flow rate of H_2 plasma pretreatment is favored in promoting the formation of uniform Ni nanoparticles. Furthermore, the enhancement of hydrogen gas [30] in plasma treatment can provide extra exciting hydrogen (H*). Herein, the Ni layer not only aggregates gradually but also etches via exciting hydrogen. This leads Ni particles to become smaller due to the support of hydrogen at the same temperature.

In order to characterize the nature of the H_2 plasma-induced nanoparticles, the cross-sectional transmission electron microscopy (XTEM) analysis was performed. As is shown in Fig. 2, the particle sizes of Ni catalyst metal layers treated by H_2 plasma etching are rather insensitive to the flow rate, with the average size being approximately 20–30 nm. Nonetheless, the apparent crystallinity and the geometric shape of the Ni catalyst particles were significantly affected by various H_2 plasma pretreatment flow rates. As is evident in Fig. 2(a) and (b), at the flow rates of 200 and 300 sccm the Ni catalyst particles are rather disordered with a broad-based shape, while at flow rate of

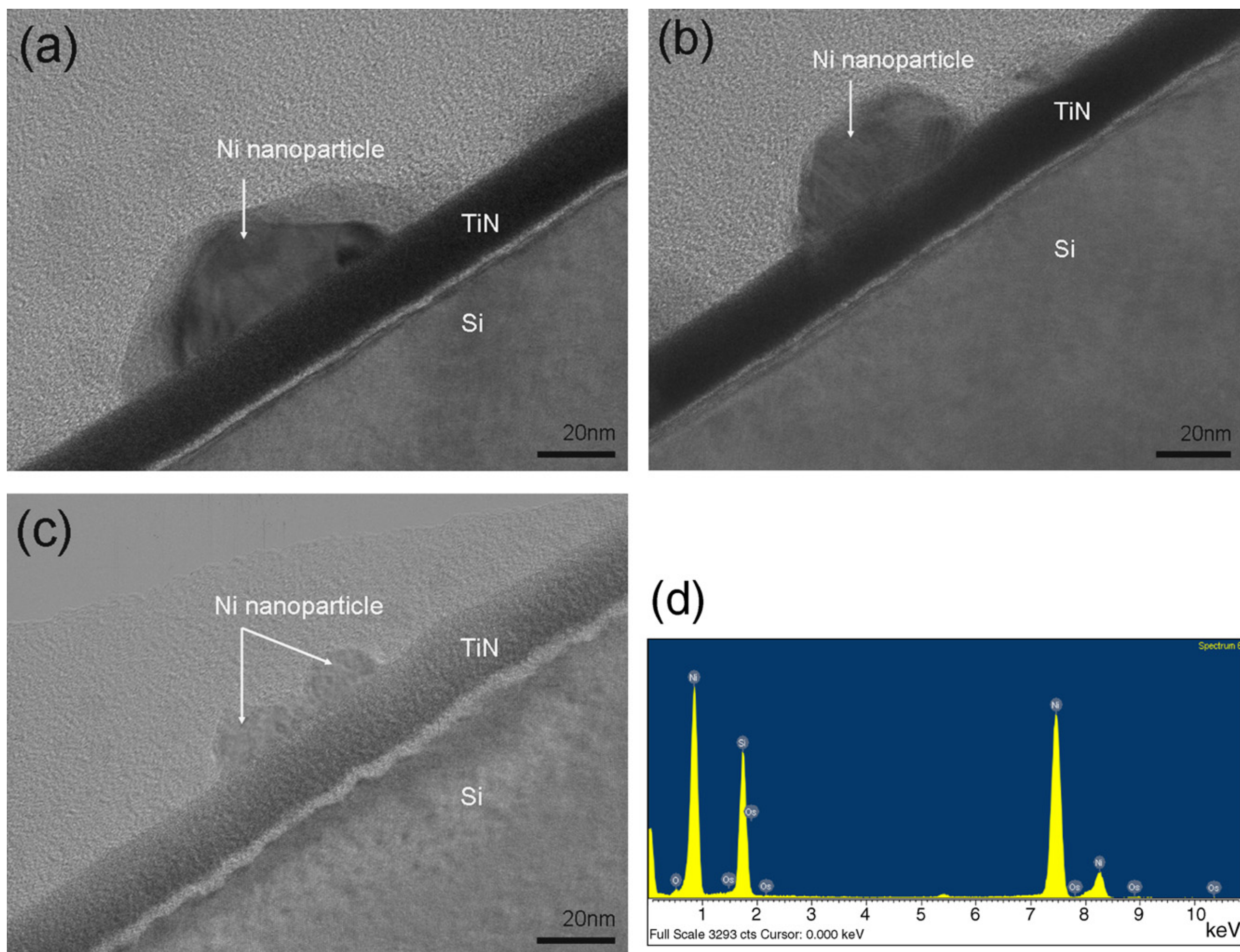

Fig. 2. TEM images of Ni catalyst nanoparticles at the various H_2 plasma pretreatment flow rates of (a) 200, (b) 300 (c) 400 sccm, and (d) the catalyst particle identified via energy dispersive X-ray spectroscopy.

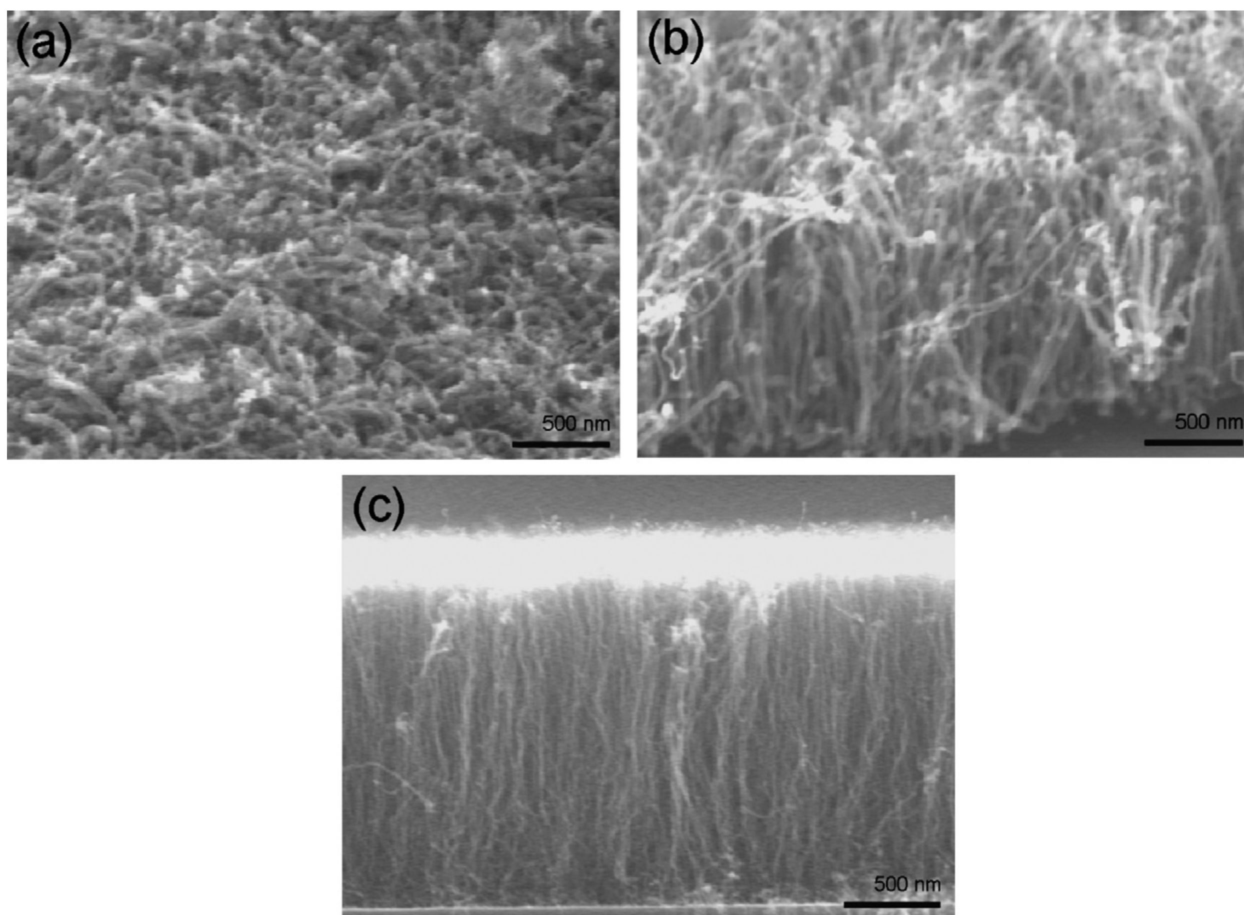

Fig. 3. SEM images of CNTs at the various H_2 plasma pretreatment flow rates of (a) 200, (b) 300 and (c) 400 sccm.

400 sccm the Ni catalyst particles (please see Fig. 2(c)) appeared to be more crystallized and have a semispherical shape. Such a morphology difference is not surprising because at the higher flow rate, the atoms in the catalyst particle can move around easier via H_2 plasma etching than at the lower flow rate. Moreover, it has also been suggested [31] that, in the plasma environment, the H_2 plasma plays a role in reducing Ni nanoparticles, and hence may also be beneficial for subsequent nucleation and growth of CNTs. Fig. 2(d) also shows that the catalyst particle identified via energy dispersive X-ray spectroscopy. This evidence can clearly present that the nickel catalyst is formed.

Fig. 3 shows the cross-sectional SEM images for CNTs grown at three synthesis flow rates: (a) 200, (b) 300 and (c) 400 sccm. It clearly demonstrates that CNTs synthesized at the flow rate of 400 sccm not only displayed the vertically aligned morphology but also exhibited much more uniform size distribution and superior aspect ratio, with the average diameter of 30–40 nm and several micrometers in length. In addition, the Raman spectra of the respective CNT samples described above (as shown in Fig. 4) also display consistent results. Briefly, the Raman spectra reflect the characteristics of some specific vibration modes. For CNTs, the two most prominent peaks in Raman spectra center at $\sim$1360 and $\sim$1580 cm^{-1} and have been frequently referred as D-band and G-band, respectively. The D-band is associated with the vibrations of carbon atoms with dangling bonds in plane terminations of ‘‘disordered graphite’’ or glassy carbons. The G-band, on the other hand, corresponds to the E_{2g} mode of graphite, and is related to the vibrations of sp^2-bonded carbon atoms in the two dimensional hexagonal lattice of the graphite layer. Consequently, the intensity of G-band, to some extent, reflects the degree of crystallinity in the graphite structure, while the intensity of D-band represents the impurities, defects or lattice distortions in CNTs.

The intensity ratio of D and G bands (I_D/I_G) is related to the size of the sp^2 carbon cluster in the graphene sheet and is nearly proportional to the defect density as proposed by Ferrari and Robertson [32]. We calculated the I_D/I_G ratio for the three CNT films pretreated by different flow rates and obtained the values of 0.98, 0.92 and 0.85 for flow rates of 200, 300 and 400 sccm, respectively. The results clearly indicate that I_D/I_G ratio decreases with increasing flow rate, suggesting that a lower degree of structural disorder could result from more intense H_2 plasma pretreatment. In addition to reducing the degree of disorder in the obtained CNTs, we note from the SEM pictures shown in Fig. 3 that higher flow rate of H_2 plasma also effectively prevents the formation of amorphous carbon and carbonaceous particles. The question is does this have anything to do with the morphology modification in the Ni catalyst particles caused by the flow rate of H_2 plasma? In order to answer this question, we tried to seek direct microstructural

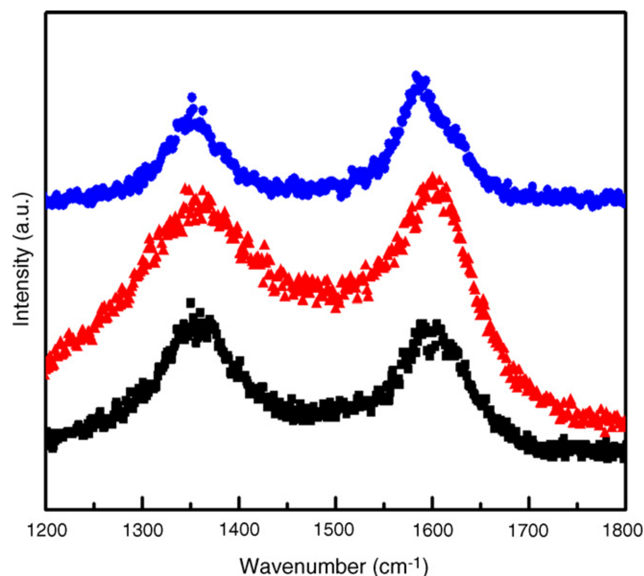

Fig. 4. Raman spectra of CNTs at the various H_2 plasma pretreatment flow rates of 200 sccm (■), 300 sccm (▲) and 400 sccm (●), respectively.

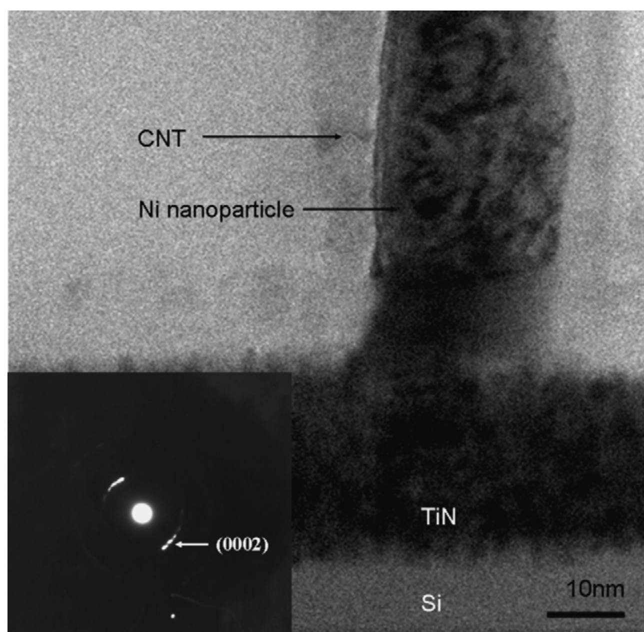

Fig. 5. TEM image of CNT synthesized at the H_2 plasma pretreatment flow rate of 400 sccm and the inset shows the SAD pattern of CNTs graphitic layers.

evidence to reveal the relevance between the structure of CNTs and the particle morphology of Ni catalyst.

Fig. 5 shows the HRTEM picture of two CNTs grown on the Ni catalyst particles treated by H_2 plasma at the flow rate of 400 sccm. The spindle-shaped Ni catalyst particle existent within the CNTs consisting of concentric graphite layers suggests that the growth mechanism of the obtained CNT might have followed that proposed by Juang et al. [33]. In addition, the inset of Fig. 5 shows the selected area diffraction (SAD) pattern [34,35] of CNTs graphitic layers. The two bright streaking spots very close to the central transmitted beam are the (0 0 0 2) basal plane reflections from the two sides of the tubule. The double split of the (0 0 0 2) reflection is due to the cone shape of the graphitic layers.

In that, an embryonic Ni catalyst particle is formed in the course of H_2 plasma pretreatment because of the difference of interfacial energies between Ni catalyst particle/substrate and Ni catalyst particle/gas. It, then, acts to enhance the catalytic decomposition of CH_4 to liberate carbon atoms. The change of elastic energy and surface energy of carbon layer caused the radius of curvature of Ni catalyst particle becoming smaller. The increased gradient of surface energy, in turn, enhances the surface diffusion of carbon atoms from bottom to the top of Ni catalyst particles. It appears that, at the higher flow rate of plasma pretreatment, the formation of the semispherical Ni catalyst particles (please see Fig. 2(c)) somehow is beneficial for the abovementioned mechanism to prevail. The details of how the morphology of the catalyst particle affects the subsequent CNT growth, however, are not clear at present and further investigations are in order.

4. Conclusions

In summary, we had combined SEM, Raman and TEM techniques to investigate the effects of various H_2 plasma pretreatment flow rates on growing CNT films on Ni/TiN/Si substrates by using MPCVD. From SEM observations, the flow rate of pretreatment plasma not only affects the density of the obtained Ni catalyst nanoparticles but also modifies their morphology. As is evident from the results of Raman spectra and XTEM observations, such changes in the Ni catalyst particles have, unexpectedly, resulted in significant effects in the morphology and crystallinity of the obtained CNTs. The observations presented here may provide a practical way of fabricating CNTs with much improved field emission characteristics.

Acknowledgments

This research was supported in part by the National Science Council in Taiwan under contract NSC 96-2112-M-009-017. Technical support from the National Nano Device Laboratories contract NDL-95S-C-067 is gratefully acknowledged.

References

[1] B.H. Chen, H.C. Lin, T.Y. Huang, J.H. Wei, H.H. Wang, M.J. Tsai, T.S. Chao, Appl. Phys. Lett. 88 (2006) 093502.
[2] Y.T. Jang, S.I. Moona, J.H. Ahnb, Y.H. Lee, B.K. Ju, Sens. Actuators B 99 (2004) 118.
[3] R. Ionescu, E.H. Espinosa, E. Sotter, E. Llobet, X. Vilanova, X. Correig, A. Felten, C. Bittencourt, G. Van Lier, J.C. Charlier, J.J. Pireaux, Sens. Actuators B 113 (2006) 36.
[4] A.S. Teh, S.B. Lee, K.B.K. Teo, M. Chhowalla, W.I. Milne, D.G. Hasko, H. Ahmed, G.A.J. Amaratunga, Microelectron. Eng. 67–68 (2003) 789.
[5] C.P. Juan, C.C. Tsai, K.H. Chen, L.C. Chen, H.C. Cheng, Jpn. J. Appl. Phys. 44 (2005) 2612.
[6] Y.H. Lee, Y.T. Jang, B.K. Ju, Appl. Phys. Lett. 86 (2005) 173103.
[7] C. Journet, W.K. Maser, P. Bernier, A. Loiseau, M.L. delaChapelle, S. Lefrant, P. Deniard, R. Lee, J.E. Fischer, Nature (London) 388 (1997) 756.

[8] A. Thess, R. Lee, P. Nikolaev, H. Dai, P. Petit, J. Robert, C. Xu, Y.H. Lee, S.G. Kim, A.G. Rinzler, D.T. Colbert, G.E. Scuseria, D. Tomanek, J.E. Fisher, R.E. Smalley, Science 273 (1996) 483.
[9] S. Fan, M.G. Chapline, N.R. Franklin, T.W. Tombler, A.M. Cassell, H. Dai, Science 283 (1999) 512.
[10] Z.F. Ren, Z.P. Huang, J.W. Xu, J.H. Wang, P. Bush, M.P. Siegal, P.N. Provencio, Science 282 (1998) 1105.
[11] Y. Huh, M.L.H. Green, Y.H. Kim, J.Y. Lee, C.J. Lee, Appl. Surf. Sci. 249 (2005) 145.
[12] J.H. Choi, T.Y. Lee, S.H. Choi, J.H. Han, J.B. Yoo, C.Y. Park, T. Jung, S.G. Yu, W. Yi, I.T. Han, J.M. Kim, Diamond Relat. Mater. 12 (2003) 794.
[13] J.S. Gao, K. Umeda, K. Uchino, H. Nakashima, K. Muraoka, Mater. Sci. Eng. B 107 (2004) 113.
[14] J.H. Choi, T.Y. Lee, S.H. Choi, J.H. Han, J.B. Yoo, C.Y. Park, T. Jung, S.G. Yu, W. Yi, I.T. Han, J.M. Kim, Thin Solid Films 435 (2003) 318.
[15] J.H. Yen, I.C. Leu, C.C. Lin, M.H. Hon, Diamond Relat. Mater. 13 (2004) 1237.
[16] W.S. Choi, S.H. Choi, B. Hong, D.G. Lim, K.J. Yang, J.H. Lee, Mater. Sci. Eng. C 26 (2006) 1211.
[17] S. Wang, P. Wang, O. Zhou, Diamond Relat. Mater. 15 (2006) 361.
[18] M. Cantoro, S. Hofmann, S. Pisana, C. Ducati, A. Parvez, A.C. Ferrari, J. Robertson, Diamond Relat. Mater. 15 (2006) 1029.
[19] Z. Chen, P.K. Bachmann, D. den Engelsen, I. Koehler, D.U. Wiechert, Carbon 44 (2006) 225.
[20] C.F. Chen, C.L. Lin, C.M. Wang, Thin Solid Films 444 (2003) 64.
[21] J.H. Han, S.H. Choi, T.Y. Lee, J.B. Yoo, C.Y. Park, T. Jung, S.G. Yu, W. Yi, I.T. Han, J.M. Kim, Diamond Relat. Mater. 12 (2003) 878.
[22] M.J. Kim, T.Y. Lee, J.H. Choi, J.B. Park, J.S. Lee, S.K. Kim, J.B. Yoo, C.Y. Park, Diamond Relat. Mater. 12 (2003) 870.
[23] H.L. Chang, C.H. Lin, C.T. Kuo, Thin Solid Films 420–421 (2002) 219.
[24] W.H. Wang, Y.R. Peng, P.K. Chuang, C.T. Kuo, Diamond Relat. Mater. 15 (2006) 1047.
[25] Y. Abdi, J. Koohsorkhi, J. Derakhshandeh, S. Mohajerzadeh, H. Hoseinzadegan, M.D. Robertson, J.C. Bennett, X. Wu, H. Radamson, Mater. Sci. Eng. C 26 (2006) 1219.
[26] J.S. Gao, K. Umeda, K. Uchino, H. Nakashima, K. Muraoka, Mater. Sci. Eng. A 352 (2003) 308.
[27] H.F. Cheng, Y. Chou, K.S. Liu, C.H. Tsai, I.N. Lin, Physica B 323 (2002) 308.
[28] T.M. Mineaa, S. Point, A. Gohier, A. Granier, C. Godon, F. Alvarez, Surf. Coat. Technol. 200 (2005) 1101.
[29] H.C. Wen, K. Yang, K.L. Ou, W.F. Wu, R.C. Luo, C.P. Chou, Microelectron. Eng. 82 (2005) 221.
[30] H. Neumayer, R. Haubner, Diamond Relat. Mater. 13 (2004) 1191.
[31] Y.H. Wang, J. Lin, C.H.A. Huan, G.S. Chen, Appl. Phys. Lett. 79 (2001) 680.
[32] A.C. Ferrari, J. Robertson, Phys. Rev. B 61 (2000) 14095.
[33] Z.Y. Juang, I.P. Chien, J.F. Lai, T.S. Lai, C.H. Tsai, Diamond Relat. Mater. 13 (2004) 1203.
[34] M.H. Kuang, Z.L. Wang, X.D. Bai, J.D. Guo, E.G. Wang, Appl. Phys. Lett. 76 (2000) 1255.
[35] M. Chhowalla, K.B.K. Teo, C. Ducati, N.L. Rubesinghe, G.A. Amaratunga, A.C. Ferrari, D. Roy, J. Robertson, W.I. Milne, J. Appl. Phys. 90 (2001) 5308.